

Multi-object reposition control of floating wind farms considering time-varying change of wind

Wei, Shangshang; Li, Zhihan; Wang, Xin; Feng, Dachuan; Gao, Xianhua

DOI

10.1016/j.oceaneng.2025.120974

Publication date

Document Version Final published version

Published in Ocean Engineering

Citation (APA)
Wei, S., Li, Z., Wang, X., Feng, D., & Gao, X. (2025). Multi-object reposition control of floating wind farms considering time-varying change of wind. *Ocean Engineering*, *327*, Article 120974. https://doi.org/10.1016/j.oceaneng.2025.120974

Important note

To cite this publication, please use the final published version (if applicable). Please check the document version above.

Copyright

Other than for strictly personal use, it is not permitted to download, forward or distribute the text or part of it, without the consent of the author(s) and/or copyright holder(s), unless the work is under an open content license such as Creative Commons.

Please contact us and provide details if you believe this document breaches copyrights. We will remove access to the work immediately and investigate your claim.

Green Open Access added to TU Delft Institutional Repository 'You share, we take care!' - Taverne project

https://www.openaccess.nl/en/you-share-we-take-care

Otherwise as indicated in the copyright section: the publisher is the copyright holder of this work and the author uses the Dutch legislation to make this work public.

ELSEVIER

Contents lists available at ScienceDirect

Ocean Engineering

journal homepage: www.elsevier.com/locate/oceaneng



Research paper

Multi-object reposition control of floating wind farms considering time-varying change of wind

Shangshang Wei^{a,*}, Zhihan Li^a, Xin Wang^a, Dachuan Feng^b, Xianhua Gao^c

- a College of Renewable Energy, Hohai University, Changzhou, 213200, PR China
- ^b Faculty of Aerospace Engineering, Delft University of Technology, Delft, 2629HS, Netherlands
- ^c School of Information and Communication Engineering, Nanjing Institute of Technology, Nanjing, 210096, PR China

ARTICLE INFO

Keywords: Floating wind farm Reposition control Drift rate Multi-objective optimization

ABSTRACT

Floating wind farms (FOWF) are one of the main forms of wind energy utilization in the deep-sea areas. This study proposes a multi-objective reposition control approach for floating wind farms. Firstly, an imperial wake model of floating wind turbines is constructed considering the effects of wind and wave conditions. A nonlinear model of a catenary mooring line is subsequently constructed. Furthermore, a multi-objective location optimization method is proposed that allows for the tradeoff between the maximum power of the farm and the minimum drift distance of the turbines accounting for the time-varying wind speed and direction. The results of the proposed approach are then compared with those of traditional methods. The findings indicate that time-varying changes in wind have a significant influence on the optimal position of turbines. It can decrease the maximum drift distance by approximately 7 % when considering temporal variations in wind. Furthermore, the proposed reposition control maintains almost the same power output of the wind farm while reducing the total offset distance from the equilibrium point of turbines by approximately 11 %. The impact of mooring orientation, natural length, turbine spacing, and wave speed on the control performance are also elucidated.

1. Introduction

The development and utilization of wind energy contributes to the sustainable development and serves as a key role in the transition to a renewable energy future (Yin and Lei, 2023; Yin et al., 2023). At present, the wind power industry is primarily classified into three categories: onshore, offshore, and deep-sea. Among these, the deep-sea area has become an inevitable trend of the wind engineering (Fox et al., 2022; Edwards et al., 2024). In addition, the utilization of deep-sea wind energy also provides a profound foundation for the future development of marine technologies (Mcmorland et al., 2022; Ojo et al., 2022). However, there are still many challenges in exploiting deep-sea wind energy. Optimal reposition control of floating wind farm is one of them (Nash et al., 2021). Reposition control leverages the coupling between the wakes of wind turbines, thereby enhancing the power of wind farms through the coordination of different turbines. Moreover, the fatigue of turbines can be reduced through control, which has a significant impact on the safe operation of wind farm (Liu et al., 2024).

For onshore wind farms, many scholars have carried out research on wake control, which can mainly be divided into the axial induction factor and vaw control (Andersson et al., 2021). The objective of the axial induction factor is to reduce the turbine power by limiting the velocity or pitch angle (Andersson et al., 2021). Yaw control is the process of adjusting the trajectory of the wake centerline of turbines and coordinating the equivalent inflow wind speed between turbines through wake offset, with the goal of improving the overall output of wind farms (Kheirabadi and Nagamune, 2019a). For bottom-fixed wind farms, the two types of control methods have been widely studied, providing a valuable basis for the optimal control of floating wind farms (López-Queija et al., 2022). Contrast to bottom-fixed technologies, floating wind turbines will drift away from their initial position, a phenomenon that has been referred to as "turbine reposition" in the literature (Fleming et al., 2015). Reposition is a critical attribute of floating turbines that differs from the fixed ones (Nagamune et al., 2023). In addition, there is a coupling between the reposition control and the yaw or pitch control (Han and Nagamune, 2020). This is because changes in the yaw or pitch of wind turbines result in modifications to the aerodynamic force, which in turn affect the movement of turbine and consequently lead to changes in the turbine's position.

From the perspective of a turbine, several studies have analyzed the

E-mail address: weishsh@hhu.edu.cn (S. Wei).

^{*} Corresponding author.

impact of drift on its performance (Han and Nagamune, 2020; Yin and Jiang, 2023). The drift not only changes the power, but also greatly affects the flow field within farm as well as the load distribution of turbines. It is evident that, in contrast to onshore wind farms, the regulation of floating wind farms is more complex due to their floating characteristics (an et al., 2017; Rodrigues et al., 2015). Some preliminary control studies therefore have been conducted for floating wind farms. In these studies, the most straightforward approach is to adjust the inflow wind speed by accounting for the impact of turbine motion, for instance, the pitch and sway. Subsequently, the conventional wake models utilized in the onshore wind farms can be employed (Ghigo et al., 2020). The disadvantage is that the temporal and spatial evolution of the wake of bottom-fixed turbines are markedly different from those of the floating type. This inevitably results in a reduction in the accuracy of this method. Therefore, studied about the wake model of floating wind turbines based on CFD have been performed. However, the complexity of actuation line models presents a significant challenge in the practical application to wind farm wake control (Yao et al., 2023; Fernandez--Rodriguez, 2023). For this reason, several scholars have adopted the fast.farm to study the impact of wake on floating wind farms (Xue et al., 2022; Rivera-Arreba et al., 2018). There are also works in developing new wake models for floating wind turbines, for instance, WFsim (Kheirabadi and Nagamune, 2021). The common routine is to complement the equivalent velocity to modify the traditional wake model. However, the impact of wave on the wake model in existing tools is not taken into consideration. Providing that empirical wake models play an important role in wind farm control due to their rapid convergence, the development of an empirical wake model for floating wind turbines is an urgent necessity.

Contrast to the numerous studies conducted on the control methodologies of onshore wind farms, there are few studies on the control for floating wind farms. The existing few studies on the control of floating wind farms exclusively focus on maximizing power output. For example, Han et al. conducted a study of the movable range of floating wind turbines in two-dimensional space under static water conditions by controlling the yaw and pitch angle (an et al., 2017). On this basis, Kheirabadi et al. maximized the efficiency of the floating wind farm by optimizing the axial induction factor and yaw angle (Kheirabadi and Nagamune, 2019b), and further analyzed the influence of wind direction and mooring characteristics on the power performance of the floating wind farm in Ref. (Kheirabadi and Nagamune, 2020).

In fact, floating wind farms are in a complex environment, and the time-varying changes in wind speed and direction cannot be avoided (Elobeid et al., 2024; Wang et al., 2023). However, existing few studies about floating wind farm control are limited to a specific wind speed and direction without considering its variation (Kheirabadi and Nagamune, 2019b, 2020). Moreover, there are dynamic response characteristics of floating wind turbines to drift (Zhang and Kim, 2018; Bashetty and Ozcelik, 2021), leading to certain limitations of the drift rate. Without considering the drift rate may cause the inaccessibility of the reposition results for engineering application. In view of this, this paper proposes a multi-objective reposition control approach for floating wind farms, which accounts for not only the temporal changes of wind speed and direction, but also the tradeoff between the maximum farm power and the minimum drift distance, thereby improving the reliability and accessibility of the optimization results.

The contributions are summarized as follows:

- A computational multi-objective reposition control approach is developed to tradeoff the maximum power of a farm and the minimum drift distance of turbines.
- The time-varying change of wind is constructed for solving the drift rate constraint issue, which is first proposed in the reposition control of floating wind farms to improve the reliability and accessibility.

The sections of this paper are as follows. The wake and mooring

models of floating wind turbines are established in Section 2. In Section 3, the control model of floating wind farms is built, and a multi-objective optimization method with maximum power and minimum drift distance is proposed. The results are analyzed in Section 4 and the conclusions are given in Section 5.

2. The simplified model of floating wind farms

2.1. Wake model of floating wind turbines

The freedom of the turbine motions should be clarified first before developing the wake model. The inertial (X, Y, Z) frame is used to measure translation displacements, i.e. surge, sway and heave, as shown in Fig. 1. The rotation of the platform is represented by the Euler angle $[\phi,\theta,\gamma]$, which corresponds to the roll angle of rotation about the x-axis, the pitch angle of rotation about the y-axis, and the yaw angle of rotation about the z-axis, respectively. Turbine wake has an important impact on the optimal control of wind farms, which not only reduces the power output of the downstream turbines, but also intensifies the fatigue. Unlike bottom-fixed turbines, floating units have multiple degrees of freedom and are affected by waves, which makes the wake model more intricate. Zhang et al. has proposed a wake model of floating wind turbines in Ref (Huanqiang et al., 2024), which considers the effects of wind shear and wave as below.

$$\begin{aligned} u(x,y,z) &= u_{ref} \left(\frac{z_0 + z_{hub}}{z_{ref}}\right)^a \left[\left(\frac{z + z_d - z_0 + z_{hub}}{z_{ref}}\right)^a - Ce^{-\frac{(y - y' + z_{hub} \sin \theta_2)^2}{2\sigma_y^2}} \right] \\ &+ u_{wave} \left[1 - Ne^{-\frac{(y - y' + z_{hub} \sin \theta_2)^2}{2\sigma_y^2}} \right] \end{aligned}$$

$$(2-1)$$

$$N = \frac{4ar_0^2}{\sqrt{2\pi}\sigma_z r_z} e^{-\frac{(z+z_d-z_0)^2}{2\sigma_z^2}}$$
 (2-2)

$$C = \frac{4ar_0^2}{\sqrt{2\pi\sigma_z}r_z}e^{-\frac{(z+z_d-z_0)^2}{2\sigma_z^2}} + \frac{a\int_{-r_0}^{r_0} \left(\left(\frac{z+z_d-z_0+z_{hub}}{z_{ref}}\right)^{\alpha} - 1\right)dz}{r_z}$$
(2-3)

$$z_d = \int_0^{x-x' + z_{hub} \cos \theta_2 \sin \theta_1} \beta dx \tag{2-4}$$

where β is wind rotor deflection angle, z_d is the offset of the wake center in z direction, y' is the offset of the wake center in y direction. Details of other parameter definition can be found in Ref (Huangiang et al., 2024).

When an upstream wind turbine yaws, the aerodynamic force causes a shift in the centerline of wind wake. However, the model proposed above does not consider the impact of yaw motion, so this paper further derives a wake model considering the influence of yaw based on the aforementioned model. This yaw is analogous to the deflection effect of conventional bottom-fixed turbines. For the spar turbine, it is assumed that the degrees of freedom associated with different rotation motions are independent of each other.

The offset of the wake centerline has a direct impact on the power output of downstream wind turbines, so the challenge in modeling yaw wake is to calculate the offset of the wake center under yaw conditions, as illustrated in Fig. 2. The thrust on a yaw wind turbine is generated by the cosine of the incident wind, and the equation is obtained by decomposing the thrust in the *x* and *y* directions:

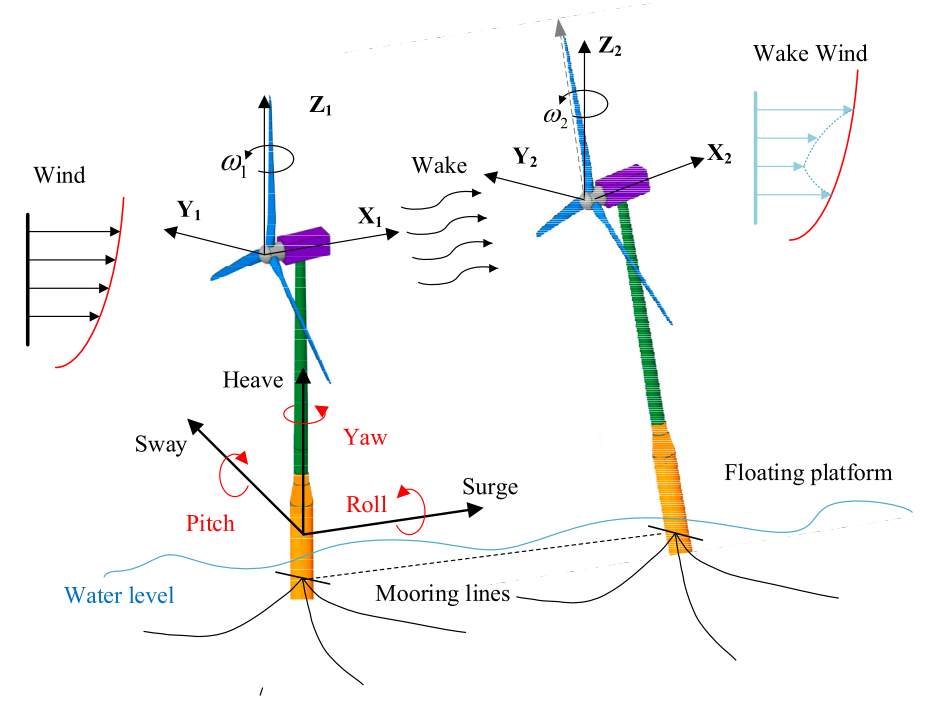


Fig. 1. Schematic wake interface of spar floating turbines.

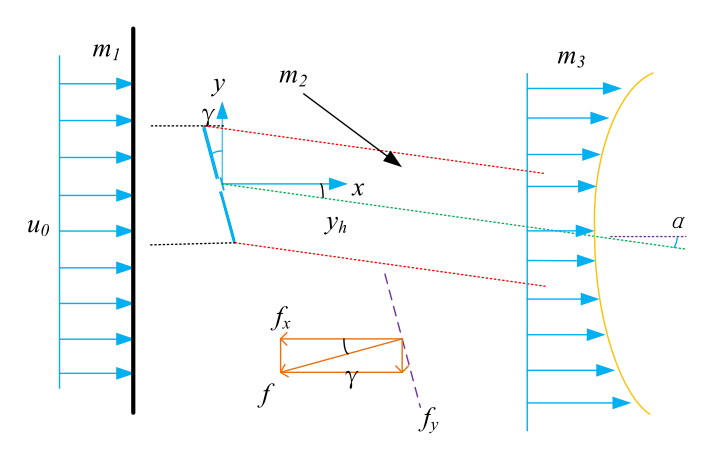


Fig. 2. Wake profile under yaw effect.

$$\begin{cases} f = C_T \cdot \frac{1}{2} \rho A (U_0 \cos \gamma)^2 \\ f_x = -f \cos \theta = -C_T \cdot \frac{1}{2} \rho A (U_0 \cos \gamma)^2 \cos \gamma \\ f_y = -f \sin \theta = -C_T \cdot \frac{1}{2} \rho A (U_0 \cos \gamma)^2 \sin \gamma \end{cases}$$
 (2-5)

In the yaw control body, the sum of the input momentum m_1 , the momentum $\log m_2$ by the turbine, and the ambient wind momentum m_3 are equal to the wind wake momentum. By applying the principles of conservation of momentum and mass, the following equations are derived:

$$\begin{cases} f_x = m_3(U_0 - \Delta U)\cos\alpha - m_1U_0 - m_2U_0 \\ f_y = m_3(U_0 - \Delta U)(-\sin\alpha) \\ m_3 = m_1 + m_2 = \int u_w dA \\ m_3 = \rho(U_0 - \Delta U) \cdot \pi r_x^2 \end{cases}$$
(2-6)

Due to the small α of the deflection angle, $\sin\!\alpha$ and $\tan\!\alpha$ can be

approximated to α , $\cos \alpha$ approximate to 1, ΔU approximate to 0, and the cross-sectional area A of the control body is also very small.

$$\alpha = \frac{-F_{y}}{\rho \int u_{w}^{2} dA} \approx \frac{1}{2} C_{T} \cos^{2} \gamma \cdot \sin \gamma$$
 (2-7)

Finally, the value of the offset yd is obtained as:

$$y_d = \int_0^x \tan \alpha \cdot dx \approx \int_0^x \alpha dx = \frac{1}{2} C_T \cos^2 \gamma \cdot \sin \gamma \frac{r_0 x}{r_0 + k_y x}$$
 (2-8)

Due to the rotation of the wind turbine in the x, y, and z directions, the reference coordinate system undergoes changes, resulting in a corresponding variation in the coordinate positions. As shown in Fig. 3, the coordinates (0,0,z) are transformed into $(zcos\varphi sin\theta cos\gamma, zsin\varphi cos\gamma, zcos\varphi cos\theta)$

$$x_0 = x' - z_{hub} \cos \varphi \sin\theta \cos \gamma \tag{2-9}$$

$$y_0 = y' - z_{hub} \sin \varphi \cos \gamma \tag{2-10}$$

$$z_0 = z' + z_{hub} \cos \varphi \cos \theta \tag{2-11}$$

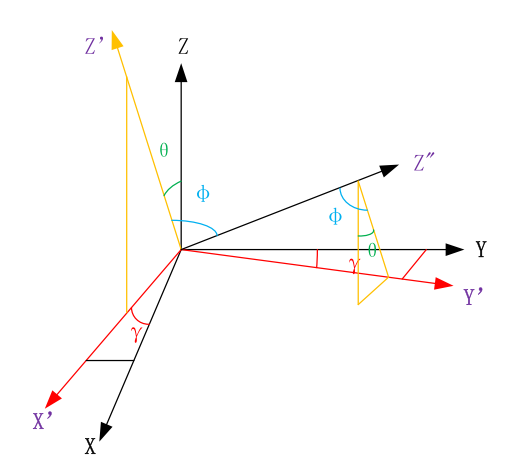


Fig. 3. Rotation angle of a floating turbine.

finally, the wake model of the floating wind turbine considering yaw is derived as below

mooring line is not on the seabed and the slope of the mooring profile at the anchors is greater than zero, it is in zone 3. The middle part is zone 2 where both horizontal and vertical forces exist on the fairlead. In this

$$u(x,y,z) = u_{ref} \left(\frac{z_{0} + z_{hub} + z_{d} - z_{0}}{z_{ref}}\right)^{a} \left[\left(\frac{z + z_{hub} + z_{d} - z_{0}}{z_{ref}}\right)^{a} - \left[\frac{4ar_{0}^{2}}{\sqrt{2\pi}\sigma_{z}}r_{z} + \frac{a\int_{-r_{0}}^{r_{0}} \left(\left(\frac{z + z_{hub} + z_{d} - z_{0}}{z_{ref}}\right)^{a} - 1\right)dz}{r_{z}}\right] e^{-\frac{\left(y - y_{d} - y_{0}\right)^{2}}{2\sigma_{y}^{2}}} \right] + u_{wave} \left[1 - \frac{4ar_{0}^{2}}{\sqrt{2\pi}\sigma_{z}}r_{z} + \frac{\left(\frac{z + z_{d} - z_{0}}{2\sigma_{z}^{2}}\right)^{2}}{r_{z}} + \frac{a\int_{-r_{0}}^{r_{0}} \left(\left(\frac{z + z_{hub} + z_{d} - z_{0}}{z_{ref}}\right)^{a} - 1\right)dz}{r_{z}}\right] \right]$$

$$(2-12)$$

2.2. Mooring model of floating wind turbines

The principal distinction between floating and bottom-fixed turbines is the mooring system. The mooring force model is contingent upon the determination of the anchor point and the connection point between the line and the pontoon. For different anchor points of a turbine, this work assumes that the mooring line is in a bisecting state. Once the projected radius Ra is specified, the coordinates of the different anchor points of the turbine can be calculated, as illustrated in Fig. 4. It should be noted that, compared with the long mooring line, the rotation of the turbine has a negligible impact on the change of the fairlead coordinates, so this paper ignores the influence of the rotational motions on the fairlead position. Under such simplification, the coordinates of the fairlead are equal to the turbine position. Therefore, for a single-point three-line mooring system, the coordinates of the anchors and fairlead can be calculated in accordance with the coordinates x and y.

Since mooring lines have some symmetry, the model of a single mooring line is the basis. As shown in Fig. 5, there are three zones of a mooring line. When the corresponding mooring part rests on the seabed, and its suspension part is vertical without a conduit profile, it is the beginning of zone 1. There is only vertical force of fairlead of the mooring when it is in zone 1. Contrast to zone 1, when any part of the

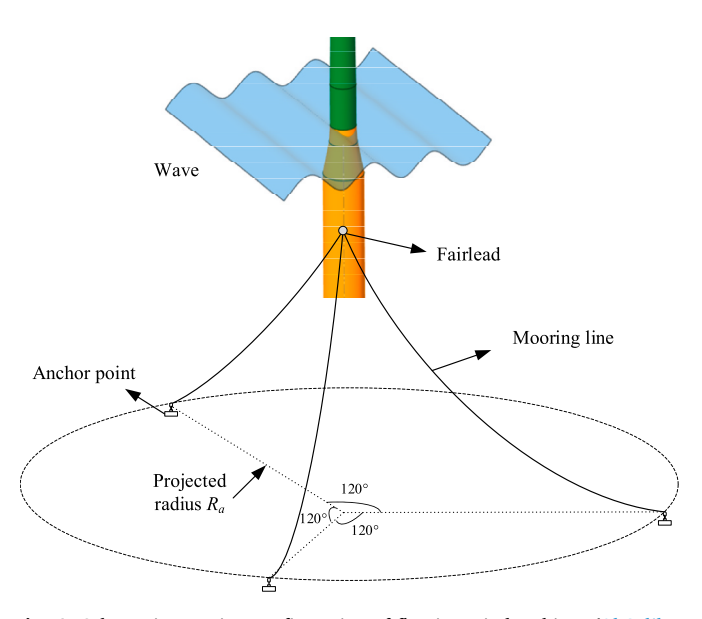


Fig. 4. Schematic mooring configuration of floating wind turbines (Al-Solihat et al., 2015).

paper, a centralized mass approach is used here and the cut-off points between different zones can be calculated as below,

$$X_{m,1} = L_{\rm c} - z_{\rm m}$$
 (2-13)

$$X_{m,2} = \frac{H_{m,2}}{w} \left| \frac{wL_{c}}{A_{c}E} + \sinh^{-1} \frac{wL_{c}}{H_{m,2}} \right|$$
 (2-14)

where L_c is the nature length of the mooring line, z_m is the vertical distance of the fairlead relative to the anchor, $H_{m,2}$ is the horizontal tension when the fairlead is located at $X_{m,2}$ that is calculated as:

$$H_{\text{m,2}} = \frac{wL_{\text{c}}}{2} \left[1 - \left(\frac{z_{\text{m}}}{L_{\text{c}}} - \frac{wL_{\text{c}}}{2A_{\text{c}}E} \right)^{2} \right] \left(\frac{z_{\text{m}}}{L_{\text{c}}} - \frac{wL_{\text{c}}}{2A_{\text{c}}E} \right)^{-1}$$
(2-15)

where w is the weight per unit mooring length, A_cE is the mooring tension per unit.

As can be seen that the two cut-off points can be calculated once the vertical distance and properties of mooring lines are given. Fairlead forces in different zones are different. When the projection distance relative to the anchor points is less than $X_{m,1}$, the horizontal force H_m is zero, while the vertical force equals to the weight of the mooring line suspended.

When the fairlead is in zone 2, the horizontal and vertical force H_m and V_m are calculated by using the Newton–Raphson algorithm to solve the following equations:

$$x_{\rm m} - L_{\rm s} = \frac{H_{\rm m}}{W} \left(\frac{V_{\rm m}}{A_{\rm r}E} + \sinh^{-1} \frac{V_{\rm m}}{H_{\rm m}} \right)$$
 (2-16)

$$z_{\rm m} = \frac{1}{w} \left\{ \frac{V_{\rm m}^2}{2A_{\rm c}E} - H_{\rm m} \left[1 - \sqrt{1 + \left(\frac{V_{\rm m}}{H_{\rm m}}\right)^2} \right] \right\}$$
 (2-17)

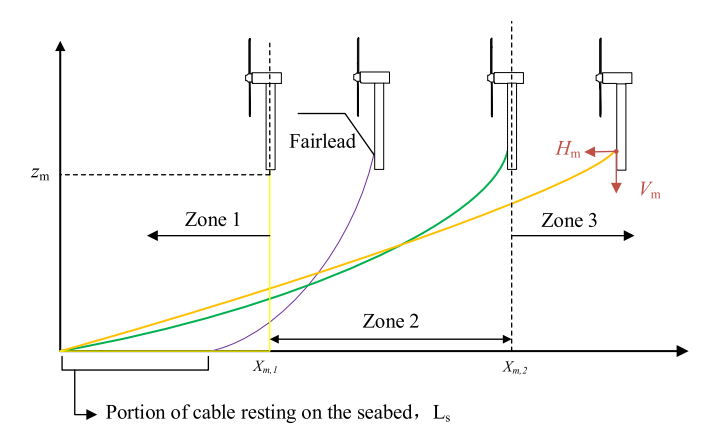


Fig. 5. Different zones of a mooring line.

where L_s is the length of the mooring line rested on the seabed, which is calculated as follows:

$$L_{s} = L_{c} - \frac{V_{m}}{w} + \frac{\left(1 + \frac{H_{m}}{A_{c}E}\right)^{3} - \left[\left(1 + \frac{H_{m}}{A_{c}E}\right)^{2} - \frac{2\mu_{s}w}{A_{c}E}x_{s}\right]^{\frac{3}{2}}}{\frac{3\mu_{s}w}{A_{c}E}} - x_{s}$$
 (2-18)

where x_s is the projection distance from the beginning of the anchors to the location with minimal horizontal mooring tension, μ_s is the resistance coefficient. This minimum mooring tension point corresponds either to the position of the anchor or to some intermediate position along the flat section. Therefore, the distance x_s is calculated as follows:

$$x_{s} = min\left[L_{c} - \frac{V_{m}}{w}, \frac{H_{m}}{w\mu_{s}}\left(1 + \frac{H_{m}}{2A_{c}E}\right)\right]$$
(2-19)

The fairlead forces in zone 3 can be calculated as below also by using the Newton–Raphson algorithm for solving H_m and V_m :

$$x_{\rm m} = \frac{H_{\rm m}}{w} \left(\frac{wL_{\rm c}}{A_{\rm c}E} + \sinh^{-1} \frac{V_{\rm m}}{H_{\rm F}} - \sinh^{-1} \frac{V_{\rm m} - wL_{\rm c}}{H_{\rm m}} \right)$$
(2-20)

$$z_{\rm m} = \frac{L_{\rm c}}{A_{\rm c}E} \left(V_{\rm m} - \frac{wL_{\rm c}}{2}\right) + \frac{H_{\rm m}}{w} \left[\sqrt{1 + \left(\frac{V_{\rm m}}{H_{\rm m}}\right)^2} - \sqrt{1 + \left(\frac{V_{\rm m} - wL_{\rm c}}{H_{\rm m}}\right)^2}\right]$$
(2-21)

It is clear that the mooring force model is strongly nonlinear. Consequently, it is computationally intensive in the optimization process if resolved every time. Therefore, the nonlinear model is solved similar to offline, and then an interpolation table function $hv_{\rm f}$ is constructed based on the results. The input to the interpolation function is the projection distance x_m , and then the table function returns the horizontal and vertical forces of the fairlead.

$$H_{\rm m}, V_{\rm m} = h v_{\rm f}(x_{\rm m}) \tag{2-22}$$

The expression depends on which zones the fairlead belongs to:

$$H_{\rm m}, V_{\rm m} = \begin{cases} 0 & , & x_m \le x_{m,1} \\ H_{\rm m,1}, V_{\rm m,1} & , & x_{m,1} < x_{\rm m} \le x_{m,2} \\ H_{\rm m,2}, V_{\rm m,2} & , & x_{\rm m} > x_{m,2} \end{cases}$$
 (2-23)

Using the interpolation table function, after the distance between the different mooring lines and anchoring positions is calculated, the mooring force can be obtained directly by interpolation, which greatly simplifies the calculation. Note that the table function only returns the forces of a single mooring line. The total mooring force is derived based on the symmetry of the mooring systems.

It should be noted that due to different anchor points of mooring

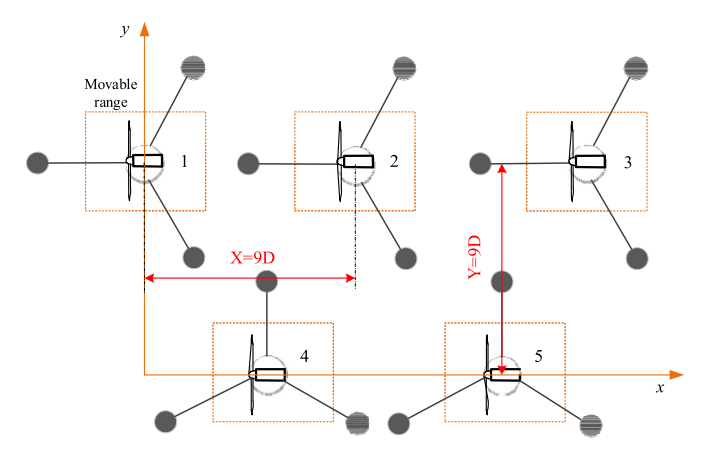


Fig. 6. Schematic layout of floating wind farm.

lines, the force of mooring lines is not the same. For the single-point three-line mooring, the vector $\mathbf{F}_{m,i,j} \in R2 \times 1$, represents a set of exponents that identify three mooring lines on given floating platform. Currently, the total mooring force of the turbine is obtained by adding multiple mooring force vectors.

$$\mathbf{F}_{\mathbf{m},i} = \sum_{j} \mathbf{F}_{\mathbf{m},i,j} \tag{2-24}$$

where m means the mooring lime, $i = \{1, 2, ..., N\}$ is the turbine number, $i = \{1, 2, 3\}$ is the number of mooring lines.

3. Muti-object wake control of floating wind farms

3.1. Layout of floating wind farm

As mentioned earlier, the purpose of reposition optimization is to adjust the wind turbine position, thereby improving the power generation of farms. At the same time, considering the time-series change of wind, the drift rate of turbines should be considered to improve the reliability and safety of the optimization results.

Taking the layout of Hywind Scotland as the reference, there are five turbines in the farm with turbine numbered as shown in Fig. 6. Due to ignoring the movement in z direction, the wind turbines are distributed on the two-dimensional sea surface. With the global coordinate system shown in Fig. 6, turbine coordinates are as follows:

$$\mathbf{X} = \begin{bmatrix} x_1 & x_2 & \cdots & x_5 \end{bmatrix}^{\mathrm{T}} \tag{3-1}$$

$$\mathbf{Y} = \begin{bmatrix} y_1 & y_2 & \cdots & y_5 \end{bmatrix}^{\mathrm{T}} \tag{3-2}$$

The actual wind speed and direction will change in time. Therefore, the temporal variation characteristics of wind are considered in this paper.

$$v_{s} = \begin{bmatrix} v_{s1} & v_{s2} & \cdots & v_{sk} \end{bmatrix}^{T} \tag{3-3}$$

$$\mathbf{v}_d = \begin{bmatrix} \mathbf{v}_{d1} & \mathbf{v}_{d2} & \cdots & \mathbf{v}_{dk} \end{bmatrix}^{\mathrm{T}} \tag{3-4}$$

where v_s is the change of wind speed, v_d is the change of wind direction, and k is the number of time instants. It should be emphasized that the wind direction here is the angle along the positive x direction counterclockwise.

Given the wind speed and wind direction, the inflow wind speed ν_i of each turbine can be obtained by using the wake model of Section 2.1, and then the power of the wind turbine can be calculated.

$$P_i = \frac{1}{2} 4a_i (1 - a_i)^2 \rho A v_i^3 \tag{3-5}$$

where a_i is the axial inducing factor of the ith turbine, A is the area of the wind turbine, and ρ is the wind density. P_i is the power of the ith turbine. The power generation of the whole farm is

$$P_{\text{farm}} = \sum_{i} P_i \tag{3-6}$$

Floating turbines can deviate from the equilibrium position, causing the mooring to stretch or shrink. Therefore, the drift distance of turbines should also be considered in the control of floating wind farms.

$$\Delta l = \sum_{i=1}^{N} \sum_{j=1}^{3} \Delta l_{ij}$$
 (3–7)

$$\Delta l_{ij} = |x_{ij} - x_{o,ij}| + |y_{ij} - y_{o,ij}|$$
 (3-8)

where $\Delta l_{i,j}$ is the drift distance, N is the number of turbines, and x_o, y_o are the turbine coordinate at the equilibrium positions, and $x_{i,j}, y_{i,j}$ are the turbine location after drift.

In addition to the overall optimization object, the physical con-

straints of each turbine itself need to be considered. Among them, the relationship between aerodynamic force and mooring force is the key to the optimization problem. For aerodynamic forces, using the temporal information of wind speed and direction, combined with the aerodynamic model in Section 2.1, the aerodynamic forces $\mathbf{F}_{t,i}$ of a turbine are shown below.

$$\mathbf{F}_{t,i} = \frac{1}{2} a_i (1 - a_i)^3 \rho A v_i^2 \begin{bmatrix} \cos v_d \\ \sin v_d \end{bmatrix}$$
 (3-9)

The mooring force, $\mathbf{F}_{m,i}$ is independent of the wind field and is entirely a function of turbine position. After the coordinates of turbines are given, the mooring force can be calculated by using the mooring force model and the interpolation table function in Section 2.2.

The wave force, $\mathbf{F}_{w,i}$ generated by ocean currents can be calculated using the Morrison equation.

$$\mathbf{F}_{\mathbf{w},i} = \frac{1}{2} C_D \rho A u_{\mathbf{w}} |u_{\mathbf{w}}| \tag{3-10}$$

where C_D is the drag coefficient, ρ is the density of seawater, A is the projected area of the unit column height perpendicular to the direction of wave propagation, u_w is the current velocity.

In existing research, given the wind speed and direction at a specific time instant, a steady-state model is used where the dynamics are not considered, in which the mooring force, the wave force and aerodynamic force are always in balance, as shown below

$$\mathbf{F}_{t,i} + \mathbf{F}_{m,i} + \mathbf{F}_{w,i} = 0 \tag{3-11}$$

In fact, wind speed and direction change dynamically. Therefore, when considering the dynamic characteristics of the wind sequence, the aerodynamics and mooring forces do not have to be always balanced, therefore a margin ϵ is required to accommodate this transition process. In this case, the aerodynamic, wave and mooring constraints that consider the dynamic change process are shown below

$$\left|\mathbf{F}_{t,i} + \mathbf{F}_{m,i} + \mathbf{F}_{w,i}\right| \le \varepsilon \tag{3-12}$$

The most important thing is that in the process of wind change, there needs time for turbines to response. Therefore, the drift rate of turbines between different moments should be considered as the following constraints. This is also the key difference between the optimization considering time-varying and those without considering the dynamics of wind.

$$\left|\mathbf{X}_{i}^{k+1} - \mathbf{X}_{i}^{k}\right| \le \delta_{\mathbf{X}} \tag{3-13}$$

$$\left|\mathbf{Y}_{i}^{k+1}-\mathbf{Y}_{i}^{k}\right|\leq\boldsymbol{\delta}_{Y}\tag{3-14}$$

where \mathbf{X}_i^{k+1} is the coordinate in x axis of the ith turbine at the k+1 time, and δ_X is the distance difference between the x coordinate at different times, and the meaning of other parameters is similar.

3.2. Optimization method of reposition control

The main purpose of traditional floating wind farms is to achieve the maximum power of the whole farm, but there will be drift of floating wind turbines. Excessive pursuit of maximum power may cause the unit to deviate far from the equilibrium position, which may affect the safety of the turbines. Therefore, the drift distance should also be considered in the reposition control of floating wind farms. A tradeoff method for a multi-object reposition control is performed. More importantly, timevarying characteristics of wind are inevitable. Consequently, the aerodynamic thrust and mooring force were relaxed when considering the change of time-series wind information, and the penalty is added in the

Table 1
Parameters for reposition control for floating wind farms (Rivera-Arreba et al., 2018; Al-Solihat et al., 2015).

Current speed	0.5 m/s	Turbine radius	63 m
Current direction	0°	Turbine power	5 MW
Water depth	186 m	Mooring	Single-point three-
		configuration	line
Natural mooring length	900 m	Tension per meter, AcE	$753.6\times10^6~\text{N}$
Radius of anchor	837 m	Offset in x, δ_X	15 m
Weight per unit length, w	1065.7 N/m	Offset in y, δ_y	15 m
x_{\max}, y_{\max}	200 m	x_{\min}, y_{\min}	-200 m

object to prevent excessive relaxation.

Finally, the optimization object in this work is as follows

$$\min_{\mathbf{X},\mathbf{Y}} \mathbf{f} = 1/P_f + \omega_1 \|\Delta \mathbf{l}\|_1 + \omega_2 \|\boldsymbol{\varepsilon}\|_1 \tag{3-15}$$

where P_f in total power generated, Δl is drift distance vector of turbines, ε is the relaxation in Eq (3–12), $\| \ \|_1$ is the L1 norm, ω_1 and ω_2 are the tradeoff coefficient.

The specific constraints are as follows

$$\begin{cases} x_{\min}, y_{\min} \leq x, y \leq x_{\max}, y_{\max} \\ Eqs (2-1) - (2-24) \\ Eqs (3-1) - (3-10) \\ |\mathbf{F}_{t,i} + \mathbf{F}_{m,i} + \mathbf{F}_{w,i}| \leq \varepsilon \\ |\mathbf{X}_{i}^{k+1} - \mathbf{X}_{i}^{k}| \leq \delta_{X} \\ |\mathbf{Y}_{i}^{k+1} - \mathbf{Y}_{i}^{k}| \leq \delta_{Y} \end{cases}$$
(3-16)

where x, y are the optimization variables, namely the turbine coordinates the constraints $x_{\min}, y_{\min} \leq x, y \leq x_{\max}, y_{\max}$ represent the moveable range from the equilibrium position of the turbine; subscript i means the ith turbine; Eqs (2-1)–(2-24) are the wake and mooring models, while Eqs (3-1)–(3-10) are the farm model. $|\mathbf{F}_{t,i}+\mathbf{F}_{m,i}+\mathbf{F}_{w,i}|\leq \varepsilon$ means the relation of force constraint. $|\mathbf{X}_i^{k+1}-\mathbf{X}_i^k|\leq \delta_X$ means the distance in x direction should be within safe range.

It is obvious that the optimization problem is a strong nonlinear problem. To solve the problem, this paper employs the sequential quadratic programming method. The overall process of the optimization process is shown in Table 2. Firstly, the environmental parameters, such as time-series change of wind, wave conditions, the mooring system parameters including the orientation, line length, and anchor points are given, as shown in Table 1. The mooring force function is then calculated offline. Given the equilibrium position of the floating turbines and the range of optimization variables, the empirical wake model was used to calculate the wind velocity, and the wind speed was used to calculate the aerodynamic thrust. Subsequently, the forces exerted on the mooring lines are interpolated based on the distance between the equilibrium position of the turbine and the mooring anchor point. The wave force can also be calculated. Then, the power of the wind farm and the total drift distance of turbines can be derived. In accordance with the objective function and constraints, the fmincon function in MATLAB is invoked to solve the problem. The use of interpolation for mooring forces (Eq (2-23)) and empirical wake models (Section 2.1) greatly simplifies the process, making it more computational efficiency.

 Table 2

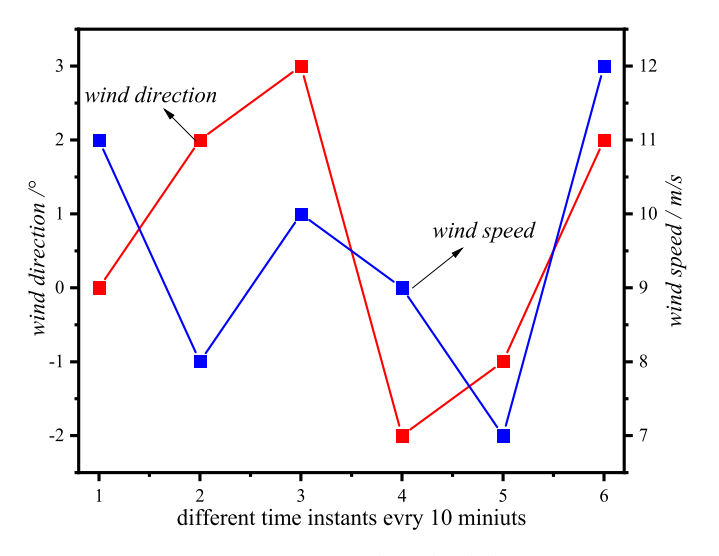
 Pseudocode of the multi-object reposition optimization.

Algorithm: Multi-object reposition control with maximizing power and minimum drift distance considering time-varying change of wind Input: Time-varying wind in Eqs (3-3), (3-4), parameters of wave, mooring and farm configuration Obtain mooring force function based on Eqs (2-13)-(2-21) Give initial turbine positions U_i←Calculate aerodynamic wake velocity based on Eqs (2-1)–(2-12) $F_{t,i} \leftarrow Calculate aerodynamic force based on Eq (3-9)$ $F_{m,i} \leftarrow$ Interpolation of mooring force table based on Eqs (2-23), (2-24) $F_{w,i} \leftarrow Calculate$ wave force based on Eq. (3-10) for each turbine Summarize power based on Eqs (3-5), (3-6) Summarize drift distance based on Eqs (3-7), (3-8) Obtain the constraints based on Eqs (3-12)-(3-14) End Construct the objection Eq (3-15) Construct the constraint Eq (3-16) Call fmincon in MATLAB for solution Output: Coordinate position of floating wind turbines Eqs (3-1), (3-2)

4. Results and analysis

4.1. Comparison of turbine location under different methods

To prove the effectiveness of the proposed method, this paper compares the results of two methods, assuming that the time-varying wind



 $\textbf{Fig. 7.} \ \ \text{Time-varying wind speed and direction.}$

speed and wind direction are shown in Fig. 7:

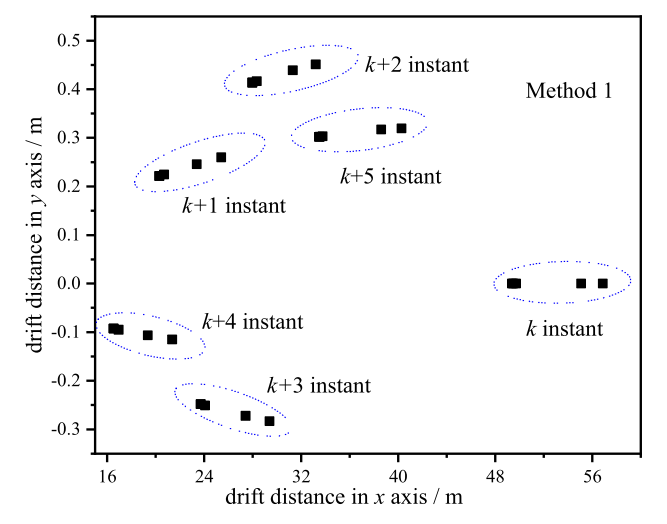
Method 1: A multi-objective optimization method without considering the characteristics of time-varying wind.

Method 2: A multi-objective optimization method considering the characteristics of time-varying wind.

Fig. 8 shows the comparison of drift distance of turbines at different time instants by the two methods. As can be seen that the overall drift trend of wind turbines is very similar, which is mainly due to the fact that the external environmental parameters are the same. However, there are also differences between different methods. For the first method, the mooring and aerodynamic force are equal at each instant without considering the relationship between different moments. This leads to larger drift distance of turbines because turbines can move freely. As demonstrated in Fig. 8 that the largest drift distance in x direction is about 57 in method 1, while it is about 53 in method 2. The maximum offset was reduced by about 7%. The difference is due to the

Table 3Comparison of total power and drift distance of wind farm under different methods.

Methods	Total power/W	Total drift distance/m
Method 1	9.35e+07	9.25e+02
Method 2	9.34e+07	8.23e+02



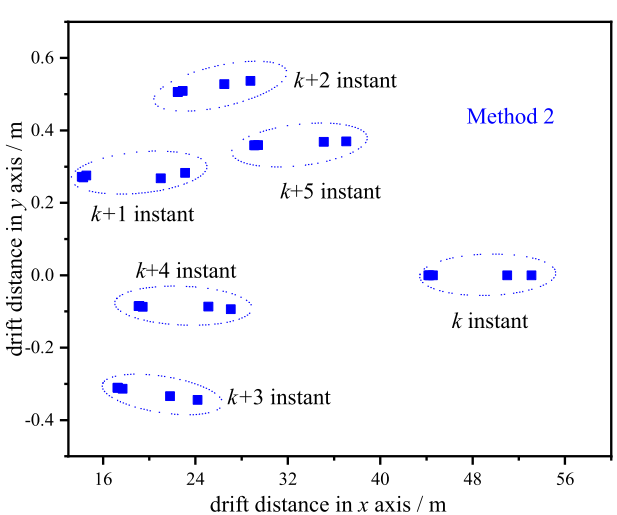


Fig. 8. Distribution of turbine drift distance at different time instant under different methods.

consideration of time-varying change of wind speed and direction. In fact, the drift distance of the first and fourth turbines is significantly reduced. The main reason for the reduction is that the dynamic response of the turbine at different times requires a certain transition process instead of reaching the equilibrium immediately. The transition process is also in line with the actual situation after considering the constraints. The optimization results demonstrate the effectiveness of the method proposed in this paper.

4.2. Comparison of total power and drift distance

The differences in turbine position led to the change of the total drift distance of turbines. The total offset distance was reduced by about 11 %, as demonstrated in Table 3. This change in drift distance is mainly from the relaxation of the balance of aerodynamic and mooring force. In addition, the drift rate also contributes to the change in drift distance. The interesting thing is that the total power of wind farms is almost the same. This phenomenon is attributed to the "overall drift" of the whole farm. Such overall drift arises from the relaxation force in Eq (3-11) in Section 3. The relaxation can be regarded as the inertial force. As a result, the turbines in Method 2 all shift a corresponding distance about 4 m. However, the relative turbine distance within the farm is almost the same in the two methods, leading to a similar wake filed of floating wind farms, thereby producing almost the same farm power.

4.3. Comparison of drift rate of turbines

It is important to note that there are distinctions between the drift distance and the drift rate. It might be helpful to think of the drift rate of turbines as showing the relationship between different time instants, while the drift distance is the movable range of turbines within certain time. Figs. 9 and 10 shows the comparison of the drift rate of turbines in x and y direction under different methods. It can be clearly seen that the drift rate of turbines in Method 1 varies according to the change of inflow wind speed without the drift rate constraints. Especially for the last time instant, the drift rates of the five turbines are all larger than the rated drift rate. However, this is infeasible in real engineering conditions, which makes it difficult to access the optimization results. In contrast, the second proposed method considers the constraints of drift rate. The drift rate of turbines in the last time instant in *x* direction is all equal the rated value, without any apparent violation of the constraints. Regarding the drift rate in y direction, the two methods yield similar results, as they both satisfy the constraints in this direction. The comparison fully demonstrates the necessity to consider the constraint of drift rates in optimization and proves the reliability of the proposed

method in this work.

4.4. Influence of mooring natural length

Fig. 11 shows the influence of mooring natural length on the overall power and the total drift distance of the wind farm. It can be seen that as the mooring natural length increases, the total drift distance increases. This is because when the natural length increases, the movable range of the turbines also increases. However, the drift distance is not that remarkable at first, because of the nonlinear mooring force. The less the mooring length is, the larger force it creates. When natural mooring length is small, the marring force is very large, resulting in the shorter drift distance. As the natural length of the mooring system increases, the mobility of the turbine also increases, which allows for larger repositioning. This enhanced mobility is beneficial for optimizing the layout of the wind farm, as it provides more flexibility in adjusting the positions of the turbines to maximize power output.

In contrast, the wind farm power decreases as the natural mooring length increases. This is because when the yaw optimization is not carried out, the upstream turbines have larger moving distance in the horizontal direction, which leads to the shortening of the relative distance between the upstream and the downstream units, leading to the increase of the wake interference effect and thereby resulting in the reduction of the farm power. This also proves the necessity for yaw control. Moreover, it can be seen that the longer the mooring line length, the greater the benefit through yaw control, which is consistent with the conclusions of existing studies (Kheirabadi and Nagamune, 2020).

4.5. Influence of mooring orientation

The mooring orientation is defined as Fig. 12 where $\theta_{\rm moor}$ is the angle between the mooring line 1 and x direction counterclockwise. Fig. 13 shows the horizontal distance of the five turbines from the equilibrium position with different mooring orientations, and it can be clearly seen that with the increasing mooring orientation angle, the horizontal drift distance of the five turbines from the equilibrium position gradually decreases and then increases, showing a symmetrical feature. This is reasonable as the mooring orientation is a single-point three lines system where the wake filed is the same for 0 and 120. When $\theta_{\rm moor}$ is 60, the force of line 1 and line 3 together resist the aerodynamic and wave force, leading to the shortest drift in x direction. As for the drift in y direction, it is because of the projection of nonlinear mooring force. This illustrates the important influence of mooring orientation on the reposition control of the floating turbines.

In addition to the offsets in the x and y directions, the orientation of

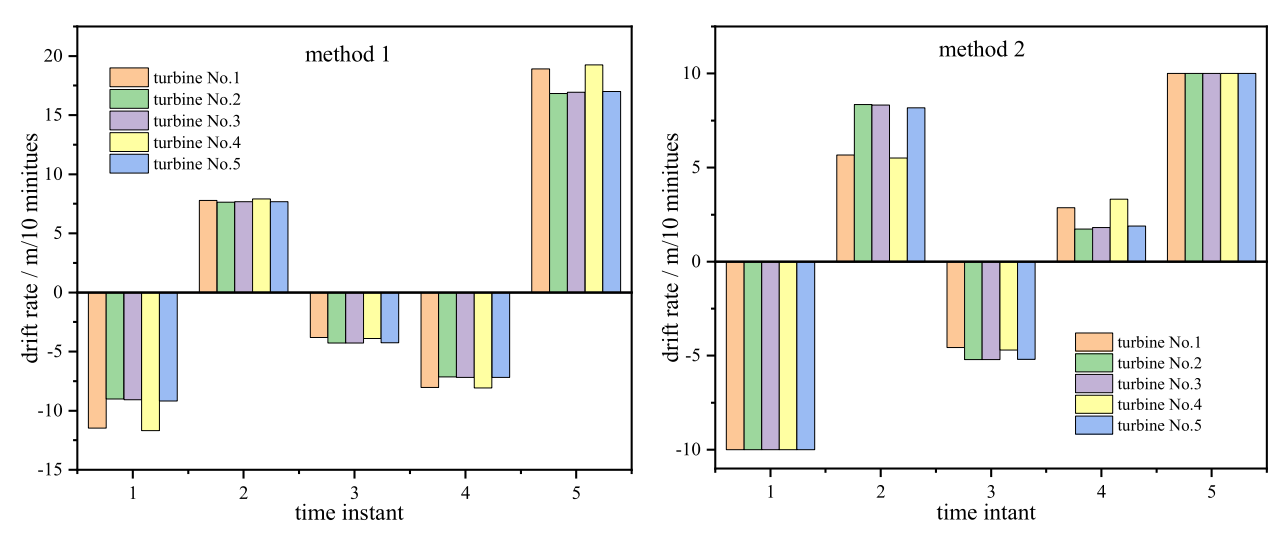


Fig. 9. Total drift rate in x direction of turbines at different time instants under different methods.

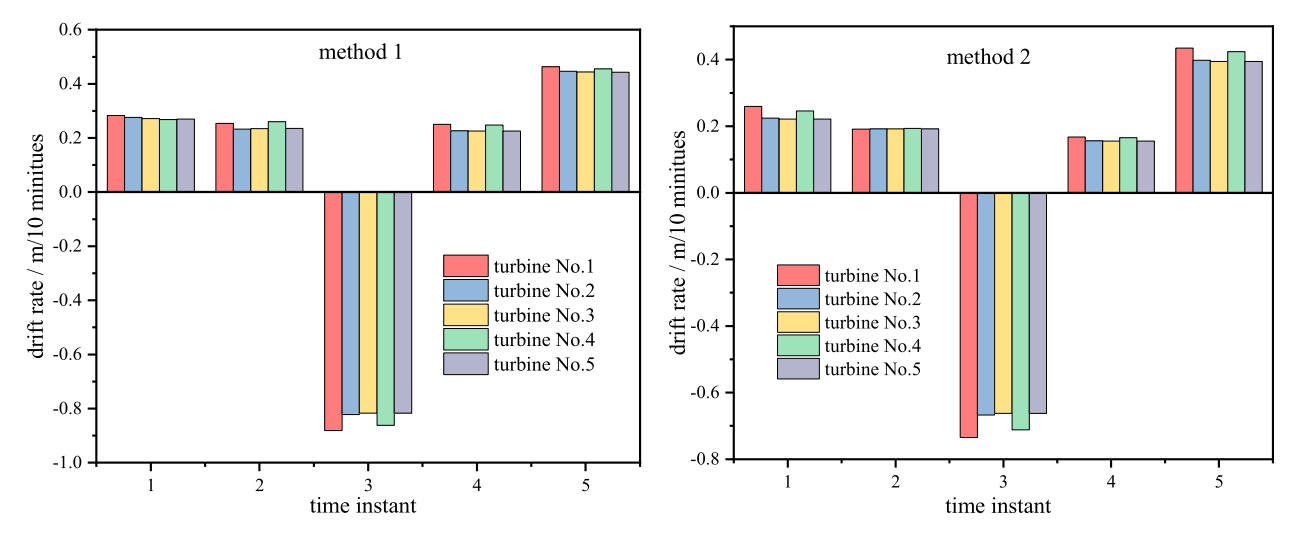


Fig. 10. Total drift rate in y direction of turbines at different time instants under different methods.

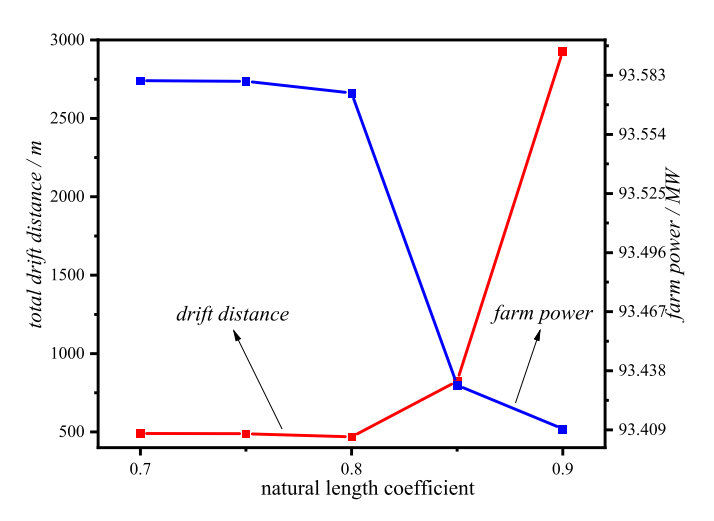


Fig. 11. Influence of mooring natural length on power and drift distance.

mooring also has great influence on the total power of wind farm as shown in Fig. 14. It can be seen that the mooring orientation has an overall symmetrical impact on the total drift distance. The symmetry characteristic of the total drift distance can be explained by Fig. 13. However, the symmetry is not observed in the total power output. This discrepancy may arise from the combined effects of the *y*-direction offset and the *x*-direction drift distance. As the orientation increases from 0 to 60° , the drift in the *y* direction of the turbines increases, while orientations between 60 and 120° exhibit a decreasing trend. Conversely, the displacement in the *x* direction follows an opposing pattern. Consequently, the total power of the wind farm is not maximized at an orientation of 60° , reflecting a comprehensive consideration of both *x* and *y* factors.

4.6. Influence of turbine spacing

Fig. 15 illustrates the influence of the turbine spacing on the control performance of the wind farm. It can be seen that as the turbine spacing

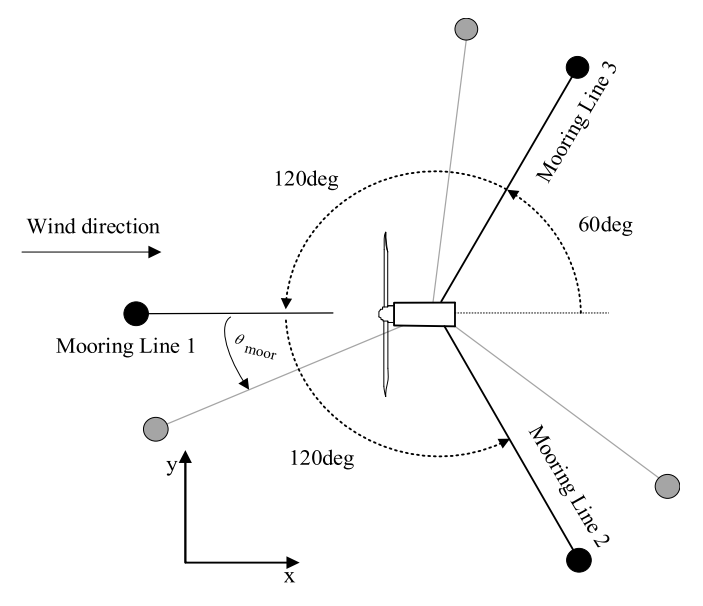


Fig. 12. Schematic of mooring orientation.

in the wind farm increases, the power of the whole wind farm increases first, and then tends to flatten. The reason for the increase is that the wake effect between the turbines is reduced as the spacing increases. However, as the spacing further increases, its influence tensity on the wind farm power decreases, because the environmental parameters and the turbine itself have not changed significantly, the impact of wake velocity change tends to be in saturation.

4.7. Influence of wave speed

Fig. 16 shows the effect of wave speed on the characteristics of floating wind farms. It can be seen that as the wave speed increases, the power of the floating wind farm decreases, whereas the drift distance increases. This is mainly due to the fact that, the horizontal force of turbines will be increased with the increment of wave speed. This will

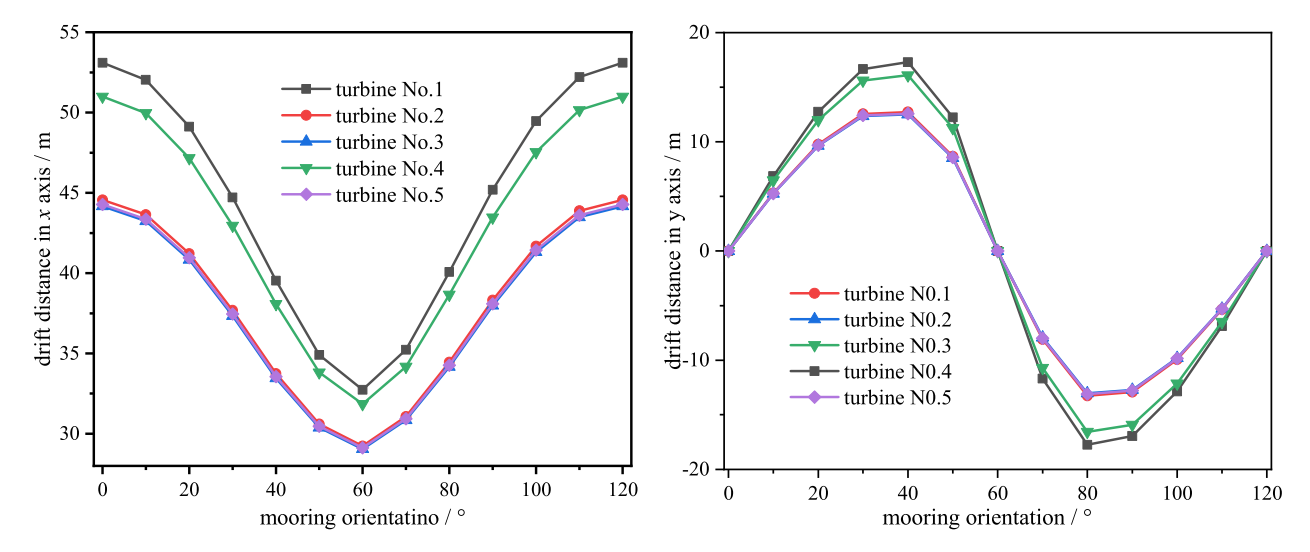


Fig. 13. Drift distance of turbines at the k time instant under different mooring orientation angles in x and y direction.

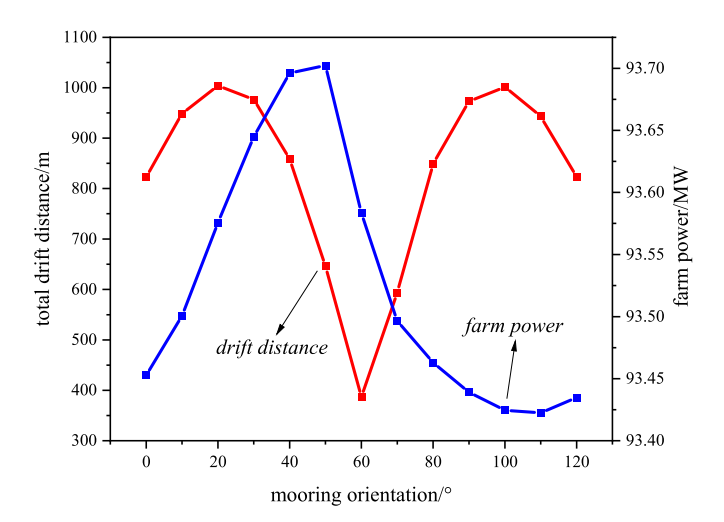


Fig. 14. Influence of mooring orientation on total power and drift distance.

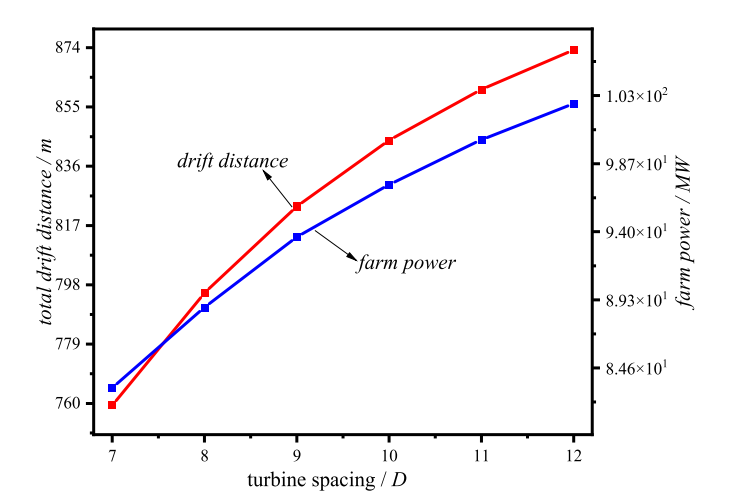


Fig. 15. Power and drift distance of wind farm under different turbine spacing.

reduce the relative turbine distance, resulting in the enhancement of the wake effect and affecting the power generation. Moreover, waves will also affect the distribution of the aerodynamic wake field, and it can be

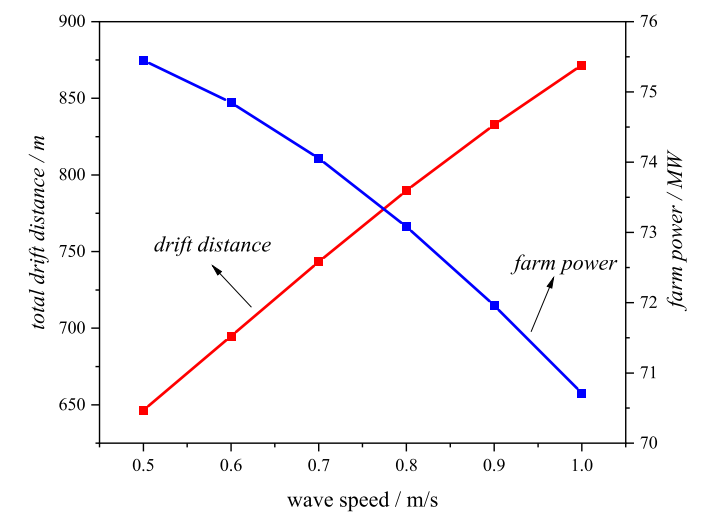


Fig. 16. Power and drift distance of wind farm under different wave speed.

seen from Eq (2-12) that the increase of wave velocity will lead to the increment of the wake velocity loss of the turbines. The dual influence of turbine position and aerodynamic wake leads to the decrease of wind farm power and the increase of drift distance.

5. Conclusions

In order to balance the efficiency and safety of floating wind farms, this paper proposes a multi-objective optimization method to achieve the maximum farm power and the minimum drift distance. Then the proposed muti-object optimization approach considering drift rate constraints is compared with a traditional method. The results show that the proposed method may be capable of producing a comparable level of power to the traditional approach. Additionally, it has the potential to reduce the overall drift distance of the turbine by approximately 11 %, which greatly improves the reliability and accessibility of the results.

Moreover, it is found that the time-varying wind is the biggest factor affecting the position of floating turbines. The augmentation of the natural length of mooring lines leads to an increase in the aggregate displacement of the turbines and a decrease in overall power output. Additionally, enlarging the inter-turbine spacing results in an escalation of both the aggregate power and the total displacement. Furthermore, an increment in wave velocity is associated with a reduction in wind farm

power and an augmentation of the drift distance. It would be beneficial to consider these parameters when performing reposition optimization of floating wind farms.

Future research endeavors should focus on resolving optimization challenges by expanding the investigation into dynamic wave models and integrating the effects of yaw control. Potential limitations to real floating wind farms include position measurement, drift rate sensors etc., which are also our further consideration.

CRediT authorship contribution statement

Shangshang Wei: Writing – original draft, Software, Methodology. Zhihan Li: Writing – review & editing, Visualization. Xin Wang: Writing – original draft, Visualization, Zhenzhou Zhao, Conceptualization, Chang Xu, Methodology, Conceptualization. Dachuan Feng: Visualization. Xianhua Gao: Visualization.

Data availability statement

The data are not publicly available due to restrictions, their containing information that could compromise the privacy of research participants.

Funding

This work is supported by National Natural Science Foundation of China (NSFC) under Grant 52406233, 52376179, 52106239, China Postdoctoral Science Foundation under Grant 2024M750738, and Fundamental Research Funds for the Central Universities under Grant 423162, Nanjing Institute of Technology University-level Scientific Research Fund under Grant YKJ202314, National Natural Science Foundation of China (No. U22B20112).

Declaration of competing interest

The authors declare that they have no known competing financial interests or personal relationships that could have appeared to influence the work reported in this paper.

References

- Al-Solihat, Khair, Mohammed, Nahon, Meyer, 2015. Stiffness of slack and taut moorings. Ships Offshore Struct. 11 (8), 890–904.
- an, C., Homer, J.R., Nagamune, R., 2017. Movable range and position control of an offshore wind turbine with a semi-submersible floating platform. AACC 1389–1394. Andersson, Leif Erik, Olimpo, Anava-Lara, Tande, John Olav, et al., 2021. Wind farm
- control Part I: a review on control system concepts and structures. IET Renew. Power Gener. 15, 2085–2108.
- Bashetty, Srikanth, Ozcelik, Selahattin, 2021. Review on dynamics of offshore floating wind turbine platforms. Energies 14.
- Edwards, Emma C., Holcombe, Anna, Brown, Scott, et al., 2024. Trends in floating offshore wind platforms: a review of early-stage devices. Renew. Sustain. Energy Rev. 193.
- Elobeid, Mujahid, Pillai, Ajit C., Tao, Longbin, et al., 2024. Implications of wave–current interaction on the dynamic responses of a floating offshore wind turbine. Ocean Eng.

- Fernandez-Rodriguez, Emmanuel, 2023. Effects of surge and roll motion on a floating tidal turbine using the actuator-line method. Phys. Fluids 35.
- Fleming, Paul, Gebraad, Pieter M.O., Lee, Sang, et al., 2015. Simulation comparison of wake mitigation control strategies for a two-turbine case. Wind Energy 18, 2135–2143.
- Fox, Harriet, Pillai, Ajit C., Friedrich, Daniel, et al., 2022. A review of predictive and prescriptive offshore wind farm operation and maintenance. Energies 15.
- Ghigo, Alberto, Cottura, Lorenzo, Caradonna, Riccardo, et al., 2020. Platform
- optimization and cost analysis in a floating offshore wind farm. J. Mar. Sci. Eng. 8. Han, Chenlu, Nagamune, Ryozo, 2020. Platform position control of floating wind turbines using aerodynamic force. Renew. Energy 151, 896–907.
- Huanqiang, Zhang, Xiaoxia, Gao, Hongkun, Lu, et al., 2024. Investigation of a new 3D wake model of offshore floating wind turbines subjected to the coupling effects of wind and wave. Appl. Energy 365.
- Kheirabadi, Ali C., Nagamune, Ryozo, 2019a. A quantitative review of wind farm control with the objective of wind farm power maximization. J. Wind Eng. Ind. Aerod. 192, 45–73.
- Kheirabadi, A.C., Nagamune, R., 2019b. Modeling and power optimization of floating offshore wind farms with yaw and induction-based turbine repositioning. Am. Automat. Control Council 5458–5463.
- Kheirabadi, Ali C., Nagamune, Ryozo, 2020. Real-time relocation of floating offshore wind turbine platforms for wind farm efficiency maximization: an assessment of feasibility and steady-state potential. Ocean Eng. 208.
- Kheirabadi, Ali C., Nagamune, Ryozo, 2021. A low-fidelity dynamic wind farm model for simulating time-varying wind conditions and floating platform motion. Ocean Eng. 224
- Liu, Yige, Zhao, Zhenzhou, Liu, Yan, et al., 2024. Combined wake control of aligned wind turbines for power optimization based on a 3D wake model considering secondary wake steering. Energy 308.
- López-Queija, Javier, Robles, Eider, Jugo, Josu, et al., 2022. Review of control technologies for floating offshore wind turbines. Renew. Sustain. Energy Rev. 167.
- Mcmorland, J., Collu, M., Mcmillan, D., et al., 2022. Operation and maintenance for floating wind turbines: a review. Renew. Sustain. Energy Rev. 163.
- Nagamune, Yue Niu, Prashant Lathi, Parth, 2023. In: Ryozo; Floating Offshore Wind Farm Control via Turbine Repositioning with Aerodynamic Force. American Control Conference (ACC), San Diego, CA, USA, pp. 2542–2547.
- Nash, Ryan, Nouri, Reza, Be-Hagh, Vasel-, Ahmad, 2021. Wind turbine wake control strategies: a review and concept proposal. Energy Convers. Manag. 245.
- Ojo, Adebayo, Collu, Maurizio, Coraddu, Andrea, 2022. Multidisciplinary design analysis and optimization of floating offshore wind turbine substructures: a review. Ocean Eng. 266.
- Rivera-Arreba, I., Eliassen, L., Bachynski, E.E., et al., 2018. Low-frequency dynamic wake meandering: comparison of FAST.Farm and DIWA software tools. J. Phys. Conf. 2021
- Rodrigues, S.F., Teixeira Pinto, R., Soleimanzadeh, M., et al., 2015. Wake losses optimization of offshore wind farms with moveable floating wind turbines. Energy Convers. Manag. 89, 933–941.
- Wang, Xinbao, Cai, Chang, Cai, Shang-Gui, et al., 2023. A review of aerodynamic and wake characteristics of floating offshore wind turbines. Renew. Sustain. Energy Rev. 175.
- Xue, Lei, Wang, Jundong, Zhao, Liye, et al., 2022. Wake interactions of two tandem semisubmersible floating offshore wind turbines based on fast.farm. J. Mar. Sci. Eng. 10.
- Yao, Tiancheng, Lu, Qi, Wang, Yipin, et al., 2023. Numerical investigation of wakeinduced lifetime fatigue load of two floating wind turbines in tandem with different spacings. Ocean Eng. 285.
- Yin, X., Jiang, Z., 2023. A novel continuously variable-speed offshore wind turbine with magnetorheological transmission for optimal power extraction. Energy Sources, Part A Recovery, Util. Environ. Eff. 45 (3), 6869–6884.
- Yin, X., Lei, M., 2023. Jointly improving energy efficiency and smoothing power oscillations of integrated offshore wind and photovoltaic power: a deep reinforcement learning approach. Protect. Control of Modern Power Syst. 8 (1), 25.
- Yin, X., Zhao, Z., Yang, W., 2023. Predictive operations of marine pumped hydro-storage towards real time offshore wind-wave power complementarity: an event-triggered MPC approach. J. Energy Storage 62, 106583.
- Zhang, Yin, Kim, Bumsuk, 2018. A fully coupled computational fluid dynamics method for analysis of semi-submersible floating offshore wind turbines under wind-wave excitation conditions based on OC5 data. Appl. Sci. 8.